Results of quality assessment tasks of the optical -electronic complex using complex instrumentation background and astroclimatic conditions

Chirov D.S., Grigoroshenko V.M.

Abstract

The report presents the results of the evaluation of the limit of instrumental performance and the quality of execution of tasks in the stages of testing and trial operation of the optical-electronic complex under complicated background and astroclimatic conditions. The dependences of the quality of problem solving of OEC from the background and astroclimatic conditions, and the boundary values of the backgrounds and characteristics of the atmosphere, in which the OEC performs tasks, for establishing an acceptable level.

***

One feature of the observations of small-sized space debris is the need to consider factors affecting the decrease in the detectability performance of the optical sensors (OS), when planning their work and in the application. These factors are astronomical-ballistic, background, and meteorological conditions in the place of the OS deployment. Accounting for these conditions during testing and operation of OS can be realized in the following ways: mathematical modeling; based on measurements of special devices (systems); combined (according to the models and measuring instruments) method. Research in this area [1, 2] showed that the most effective way to account for astronomical-ballistic, background, and meteorological conditions during testing and operation of the OM, is the combined method. Adoption of this approach has been carried out with the optical-electronic complex (OEC) "Zelenchuk" since 2007. As a result of the use of a hardware-software complex (HSC), accounting for the astronomical-ballistic and background conditions in the software algorithms and the complex special equipment estimates the limit of the instrumental characteristics and the quality of the HSC tasks in difficult background and astroclimatic conditions.

The work of the HSC accounting for the astronomical-ballistic and background conditions can be divided into two stages.

At the **first (**preparatory**) stage,** before the observations, it calculates a limiting power of the sensor at each point in the sky through the whole observation period of the date. For this it takes into account the phase illumination of the sky domains, brightness of the sky background, the decrement of the signal level due to atmospheric absorption, the decrement of the acquisition threshold due to moonlight, and some other causes.

The fall of the signal D (magnitudes) as a function of the phase angle, reducing the detection threshold M_c (given the sky background of 21 magnitudes/sq.deg.) due to changes in the brightness of the sky background illumination M_m by the Moon, or other causes, was estimated for HSC in the computational method. Reduction of the detection threshold is calculated in accordance with the expression [2]:

$$\Delta M = \frac{21 - F_f^{real}}{2}, \qquad (1)$$

where ΔM - lowering the threshold of detection (limiting power) OEC, F_f^{real} - the real value of the sky background.

To estimate the signal decrease, D, as a function of the phase angle, a priori information about the brightness of the space objects and its overall dimensions, obtained from the control center, is used.

According to the results of calculations, a table of values of the limiting power of the sensor depending on the coordinates of the elevation, azimuth, and time is prepared. The result is a map of the projected visibility the satellites. When planning work, the optical sensors for the detection of small space debris use selected areas, in which a limiting power is maximal.

Simultaneously with the calculation of the visibility maps at this stage, estimate is made of the probability of the absence from the line of sight of the OEC-satellite cloud formations, using the forecast of cloud cover in the location of the OEC.

A vertical section of the cloud field and the corresponding model screen with nontransparent ($Z(x)=0$) and the transparent areas ($Z(x)=1$) in the plane H_a is shown in Figure 1.

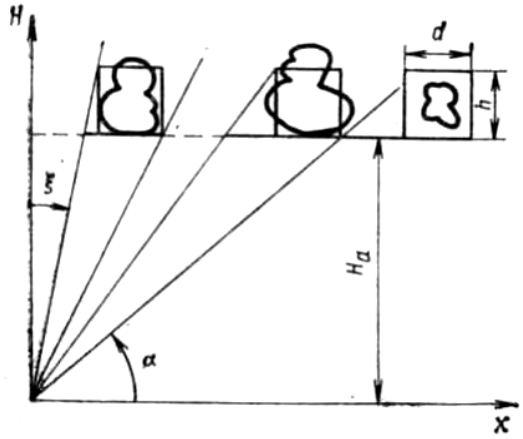

Figure 1 - The model of cloud heterogeneities.

In this case, the transmission of the field in a given direction, ξ, depends on the spatial structure of the field and is a random value. When the selected model transmission cloud field shows no clouds in the line of sight, it can be compared to the probability, that a random arrangement of the optical zone of the contact in the field of the cloud intersect with the line of sight to the screen, hits the site with $Z=1$. This probability is equal to the ratio of the area of transparent sections of the optical contact area to the whole of its area, A. If you have two shades of transmission $Z(r)=\{0,1\}$, where $r=\{x,y\}$, and x,y - coordinates in the rectangular coordinate system, the probability of the product is determined by the average passing over the area, A, of the zone, Ω_a

$$\widetilde{Z}_a=\frac{1}{A}\int_{\Omega} Z(r)dr. \qquad (2)$$

For the Poisson distribution centers of cloud heterogeneities (with only their two-dimensional structure) at $A\to\infty$ are

$$\widetilde{Z}_a=e^{\left\{-2\pi\mu_d\int_0^{\infty}[1-F(x)]rdr\right\}}, \qquad (3)$$

where μ_d - density of the filled area of cloud centers; $F(r)$ - distribution function of the size of the horizontal cloud heterogeneities. When the size of cloud heterogeneities are identical, it follows from (2) $\widehat{Z}_a = e^{(-\mu_d \pi d^2/4)}$. The average transmittance, Z_a, of the cloud field corresponds to that used in meteorology the absolute cloud grade j_a, which is associated with it as $Z_a = 1 - j_a/10$. The averaged transmittance, Z_a, characterizes the probability of the product in "windows" ($Z = 1$) cloud cover on the satellite line of sight, which is fixed and passes near the zenith ($\xi << 1$ on Figure 1). At angles $\xi > 1$ to consider three-dimensional cloud formations, $Z(\xi)$, for which the average transmission, consistent with a relative grade of meteorology, j, is

$$\widetilde{Z} = \int_0^{\pi/2} P(\xi) \sin \xi d\xi \tag{4}$$

where $P(\xi) = \widetilde{Z}(\xi) = e^{\left(-\mu_d \pi d^2/4 + 2dhtg\xi\right)}$ - probability of absence of clouds in the line of sight through the "window" of transparency in a given direction ξ; the parameters $\mu_d, d\ u\ h$ are a function of the grade of clouds, j.

The value $\widetilde{Z} = \widetilde{Z}_j$ characterizes the probability that the product in an arbitrary direction is unknown, ξ, and is associated with a relative grade of cloudiness, j, over the area as

$$P_{ATM} = \widetilde{Z}_j = 1 - j/10. \tag{5}$$

The likelihood of work OS in a given direction is define by (5), as

$$P_{ATM}(\xi) = \widetilde{Z}_j \sin \xi = (1 - j/10) \sin \xi. \tag{6}$$

The relative grade, which has grades from 0 to 10 in increments of one point, determine if ground-based observations are possible.

At the **second stage,** the model accomplishes a dynamic correction of the chart in real time by data from the Sky Monitoring System (SMS) at the facility

location. SMS provides a calculation of the cloudiness density distribution, angular rate, and direction of the cloudiness field motion, detection and prediction of the clear spaces dynamics, estimation of the atmosphere transparency coefficient value and its distribution all over the sky, and an estimate of the optical sky background level distribution. SMS uses a special object-glass of the “fish eye” type and the radiation receiver with a CCD matrix, which obtains a high resolution image (see Figure 2). All these operations are automated and the data base of sky images is used.

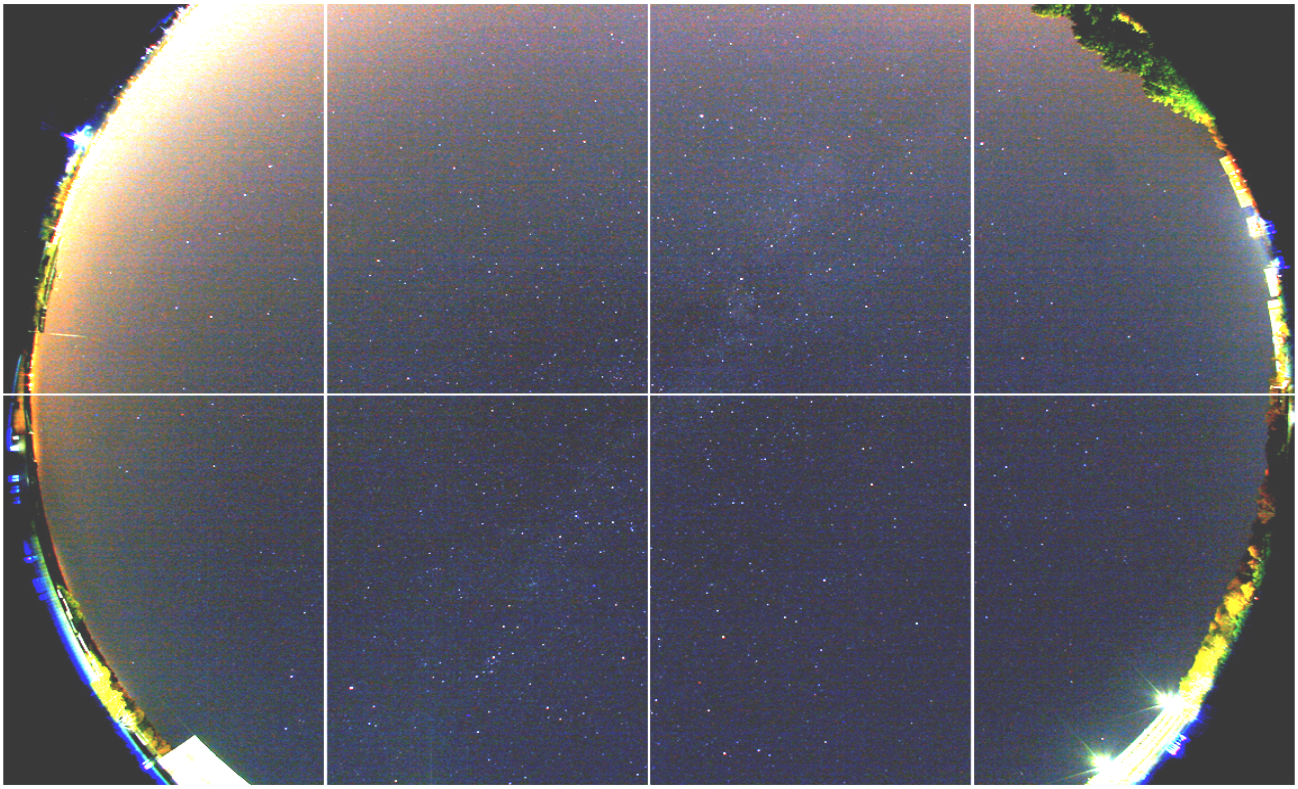

Figure 2 – Image of the sky

The estimate of the atmosphere transparency coefficient value and its distribution over the sky, and the estimate of the optical sky background level distribution are made using the photometric catalog of stars in the image of the sky.

The determination of the presence and distribution of clouds in the sky, speed, and direction of movement of the clouds, detection and prognosis of the dynamics of gaps in the cloud field, the adjustment value $P_{ATM}(\xi)$ ae made in the automated mode using a database of images of the sky. The determination of the presence and distribution of clouds are made by the separation of the sky brightness fluctuations

in the image by way of contrasts, in particular the method of Roberts, which consists in carrying out the operations of two-dimensional discrete differentiation [3]:

$$I_R(j,k) = \sqrt{\left([I(j,k) - I(j+1,k+1)]^2 + [I(j,k+1) - I(j+1,k)]^2\right)}, \qquad (7)$$

where $I(j,k)$ - the brightness value of image pixel coordinates (j,k). Roberts' method is to perform two linear operations of differentiation in various directions at an angle of 45°.

Determination of the angular rate and direction of the cloudiness field motion, and detection and prediction of the clear spaces dynamics are performed by analyzing the dynamics of the change in the optical state of the sky from the images obtained from the database, and the values of the wind speed and direction at the appropriate heights. According to the results of SMS an operational map of satellite visibility is made.

Simultaneously with the work of SMS there is an assessment of the meteorological conditions at the site of deployment of OEC: wind speed and direction, and parameter Cn^2. These estimates, together with a map of the satellites visibility, are used to adjust the operational plans of the OEC, in order to achieve the best accuracy and quality measurements.

One of the important parameters affecting the quality of OEC functional tasks, estimated in the second stage of the HSC, is the probability of obtaining an optical image with high angular resolution. This parameter, P_{oi}, is evaluated in accordance with [4]:

$$P_{oi} \approx 5.6 \exp\left[-0.1557 \cdot \left(D/r_0\right)\right], \qquad (8)$$

where D - aperture diameter, r_0 - Fried parameter. Equation (8) is valid for $D/r_0 \geq 3.5$.

The probability of obtaining an optical image with high angular resolution is carried out promptly (before the start of a session of observation) of the evaluation r_0. This information allows the operator to take the OEC with the feasibility of

obtaining optical images in the session. Table 1 presents estimates of the probability of obtaining a quality optical image, depending on the parameter D/r_0 [4].

Table 1

D/r_0	P_{oi}
2	0.986±0.006
3	0.765±0.005
4	0.334±0.014
5	$(9.38\pm0.33)\times10^{-2}$
6	$(1.915\pm0.084)\times10^{-2}$
7	$(2.87\pm0.57)\times10^{-3}$
10	$(1.07\pm0.48)\times10^{-6}$
15	$(3.40\pm0.59)\times10^{-15}$

Analysis of the work of the HSC in 2011 led to the following conclusions:

40% of the time the wind speed at the site of the location OEC is 3 m/s and above (see Figure 3), which does not allow high-quality optical images. In these times, OEC should be used for angle and photometry measurements;

for the period analyzed, OEC observations of satellites would be under the cloud cover about 46% of the time (see Figure 4);

conditions of atmospheric turbulence, allowing to obtain optical images, with maximum angular resolution, on the order of 19% of the analyzed time period (see Figure 5). The probability of obtaining high-quality images is of the order of 0.76 ... 0.82.

Reference:

1. Михельсон Н.Н. Оптические телескопы. Теория и конструкция. – М.: Наука, 1976.

2. O.Aksenov, S.Veniaminov, A.Rykin, D.Chirov. Some results of testing the model for taking into account astro-ballistic and sky-background conditions when planning space debris observations // 27 session of IADC, Darmstadt, Germany, 2009.

3. Лучин А.А., Тимошенко А.С., Перевозчиков Н.И., Чиров Д.С. Информационные технологии обработки оптических и радиолокационных изображений в задаче распознавания космических аппаратов // «Информационные технологии», № 11, 2004 г, Москва.

4. David L. Fried. Probability of getting a lucky short-exposure image through turbulence // J. Opt. Soc. Am., Vol. 68, No. 12, December 1978, pp.1651-1658.

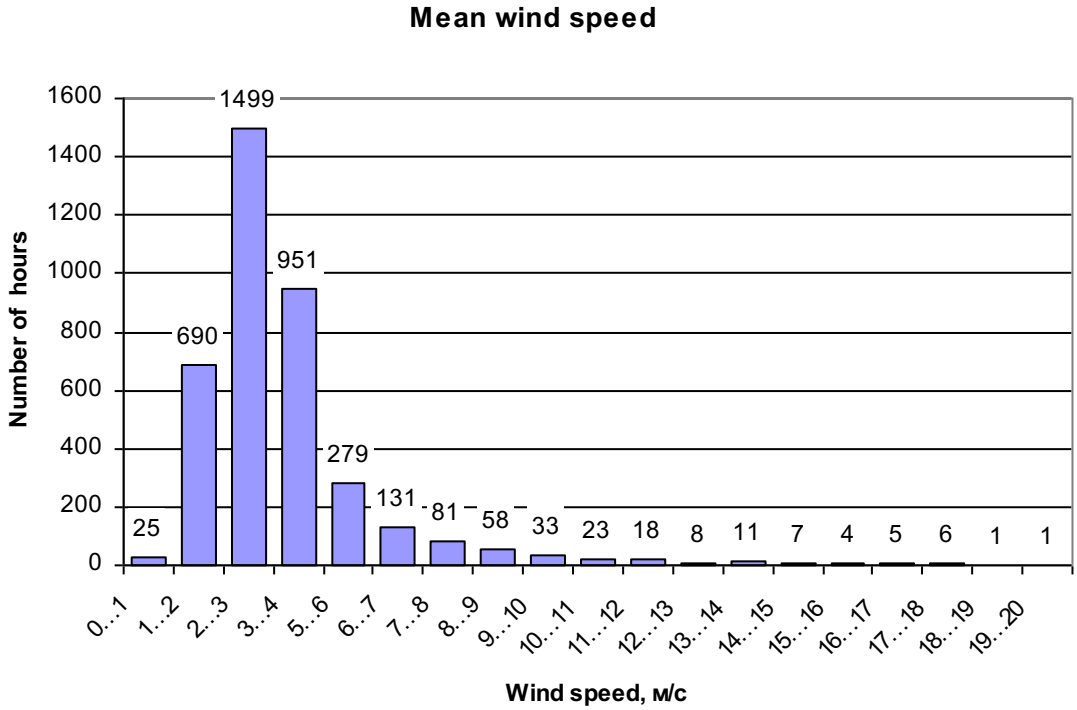

Figure 3

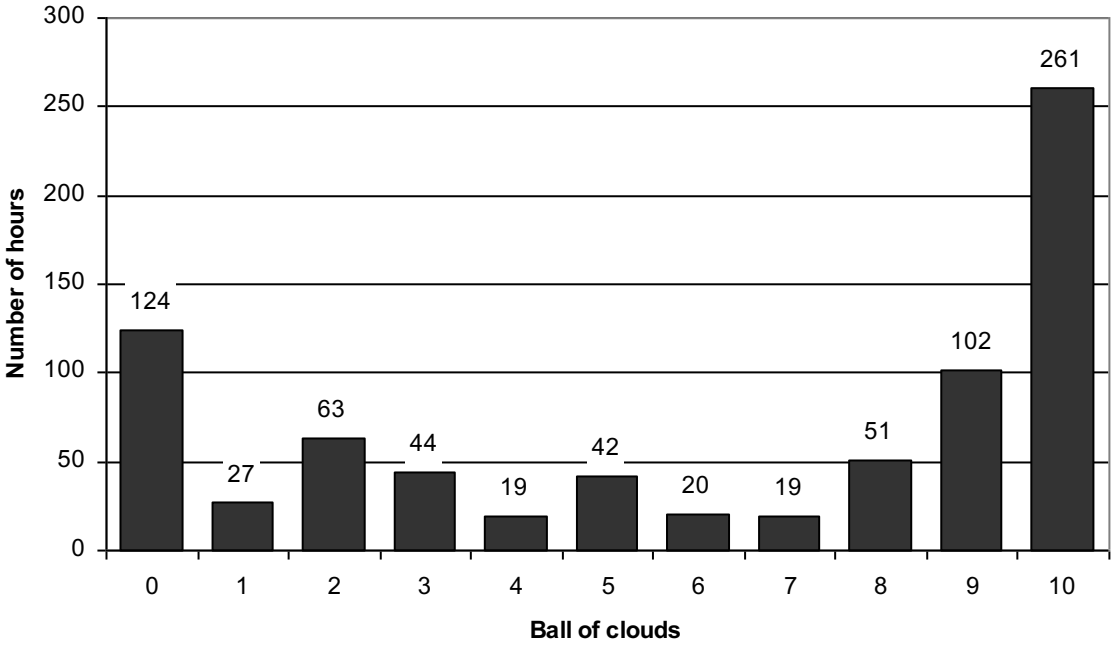

Figure 4

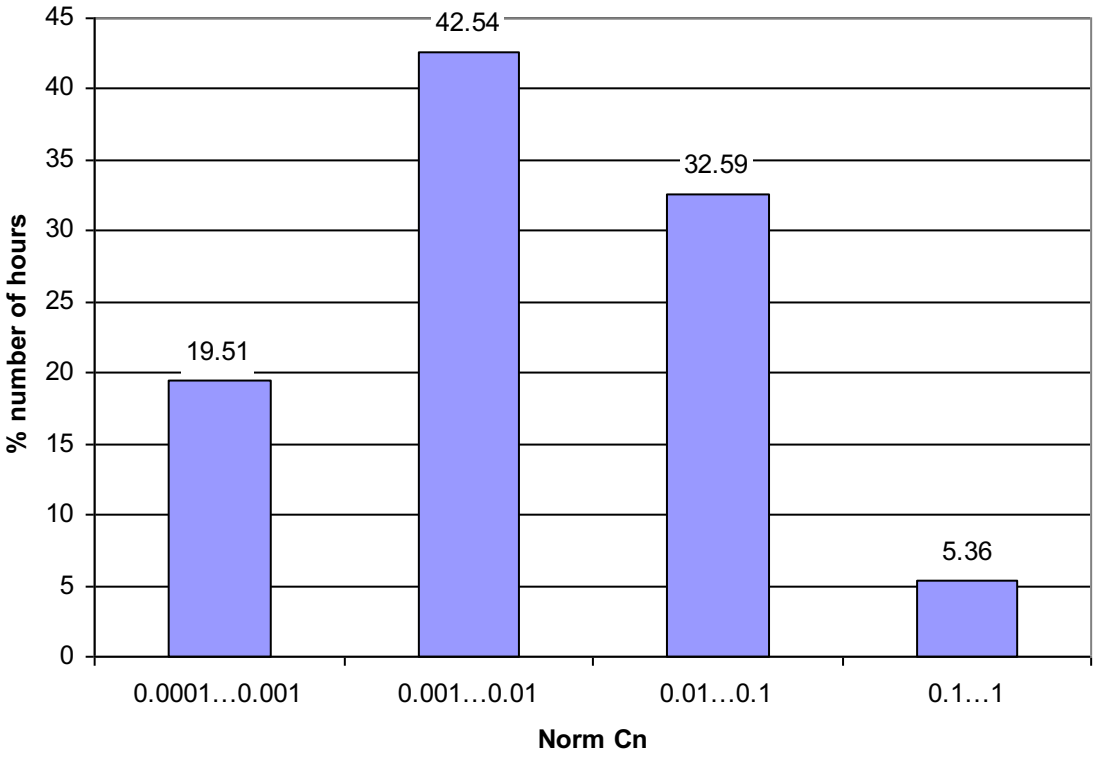
45
40
35
30
25
20
15
10
5
0
% number of hours
42.54
32.59
19.51
5.36
0.0001…0.001
0.001…0.01
0.01…0.1
0.1…1
Norm Cn

Figure 5